MEASUREMENTS OF PRODUCTION AND DISTRIBUTION OF RADIONUCLIDES IN THE SPALLATION TARGET

Władysław Pohorecki, Jerzy Janczyszyn, Stefan Taczanowski
University of Mining and Metallurgy, Faculty of Physics and Nuclear Techniques
Al. Mickiewicza 30, 30-059 Cracow, Poland,
pohorecki@novell.ftj.agh.edu.pl

Aleksander Polanski
Joint Institute of Nuclear research, Laboratory of Information Technologies
Dubna, Russia
polanski@jinr.ru

ABSTRACT

Designing of an Accelerator Driven System needs a thorough evaluation of build-up of long-lived radioactivity and changes in elemental composition in construction materials. They can be calculated with the use of experimentally verified computer codes and data libraries. The experiment presented here is thought as a part of such verification. Samples of Pb and Bi were placed respectively in and behind a Pb target irradiated with 650 MeV protons. Gamma spectra of samples were counted and analysed. Activities of several radionuclides were determined and some of them compared with values obtained from MCNPX calculations.

1. INTRODUCTION

In a real accelerator driven system (ADS) transmutations, which occur in construction materials composing the target and its surroundings, lead to a build-up of long-lived radioactivity and to changes in elemental composition of these materials. Precise evaluation of the effects in a long time of exposition can only be done by calculation with the use of experimentally verified proper computer codes and data libraries. The presented below experiment is thought as a part of such verification, especially for the calculation of target materials transmutation and induced radioactivity. They were carried out in the frame of a larger project called SAD (from Subcritical Assembly in Dubna).

Samples were placed inside and on the surface of cylindrical (Φ80×500 and Φ80×308 mm) natural Pb targets which has been irradiated with protons. Description of the longer target end respective experiment are given elsewhere [1]. Aluminium monitors were applied for the sake of monitoring the absolute total number of protons in the beam and for the assessment of the beam shape. Gamma spectra of irradiated samples were counted with the use of semiconductor detectors and analysed to identify produced radionuclides, determine their activity and its spatial distribution. The distributions determined experimentally were compared with respective ones calculated with the use of LAHET and/or MCNPX codes.

2. EXPERIMENTAL CONDITIONS

In addition to the target the equipment for conducting the experiment included JINR 660 MeV proton accelerator [2] and HPGe gamma spectrometers.
The values of parameters applied in the experiment were:

- proton energy: $E_p = 650 \pm 4$ MeV
- max. proton yield: $I_{p,max} = 3 \cdot 10^{10}$ p/s,
- irradiation time $t_i = 20$ m - 3 h,
- min. decay time $t_{d,min} = 10$ h.

The spallation target consisted of several 5 cm and 1 cm thick cylindrical parts and 31 pieces of 1mm thick lead samples all 80 mm in diameter (Fig.1). The Pb samples were placed along the target in such a way that to best reproduce the characteristic distribution of proton induced activity of Bi radionuclides evaluated earlier with the use of LAHET code. The total length of the target was 308 mm.

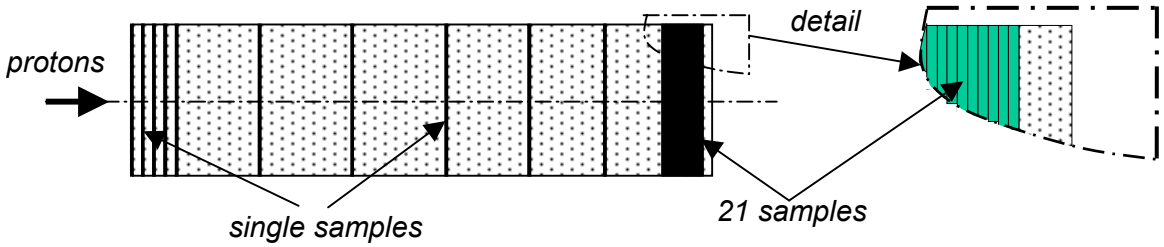

Fig. 1. Composition of the lead target. Diameter - 80 mm, length - 308 mm. Sample thickness - 1 mm.

Small samples of elements composing ADS construction materials were fixed in a polyethylene holder and placed at the front and at the end of the target (Fig.2). From those samples only the results obtained for the Bi once placed behind the target are presented in this paper.

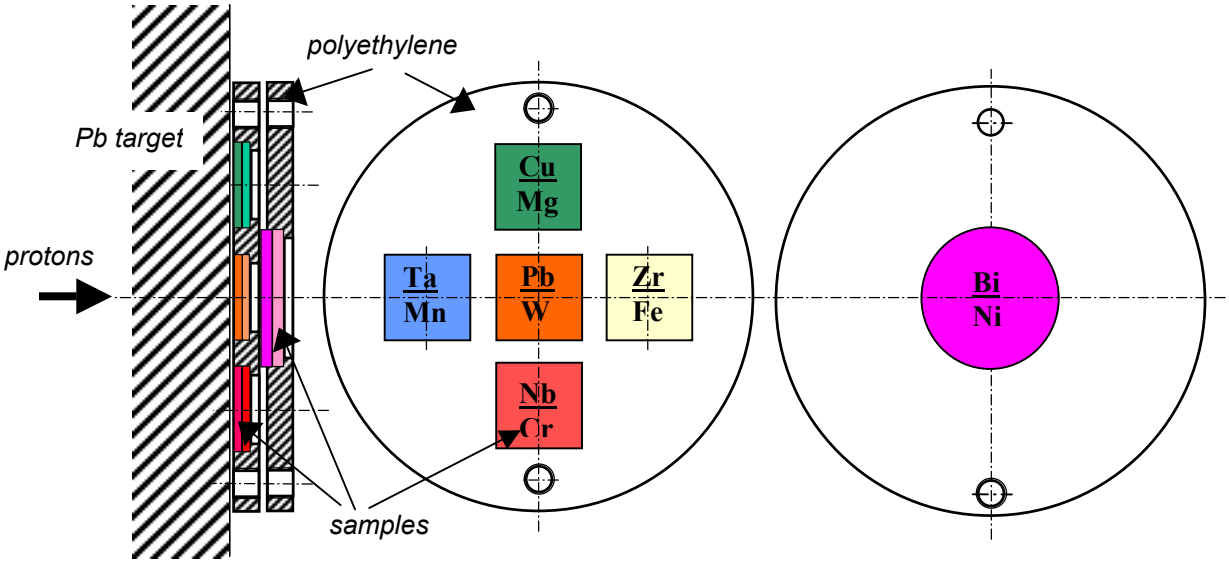

Fig. 2. Positioning of samples in the sample holder at the end of target

The samples dimensions were Φ18 mm × 1 mm. All target parts and samples together with proton monitors were placed in a special aluminium holder (Photo 1a). Thin (8.41 mg/cm^2) 99.99% Al foils 85 mm in diameter and the ^{27}Al(p,x)^{22}Na reaction were applied for monitoring the total number of protons hitting the target during irradiation. The distribution of proton intensity on the beam cross section i.e. the beam profile was assessed with the use of 8×8 matrix of Al samples 5×5×0.5 mm^3 each (Photo 1b) and ^{27}Al(p,x)^{24}Na reaction.

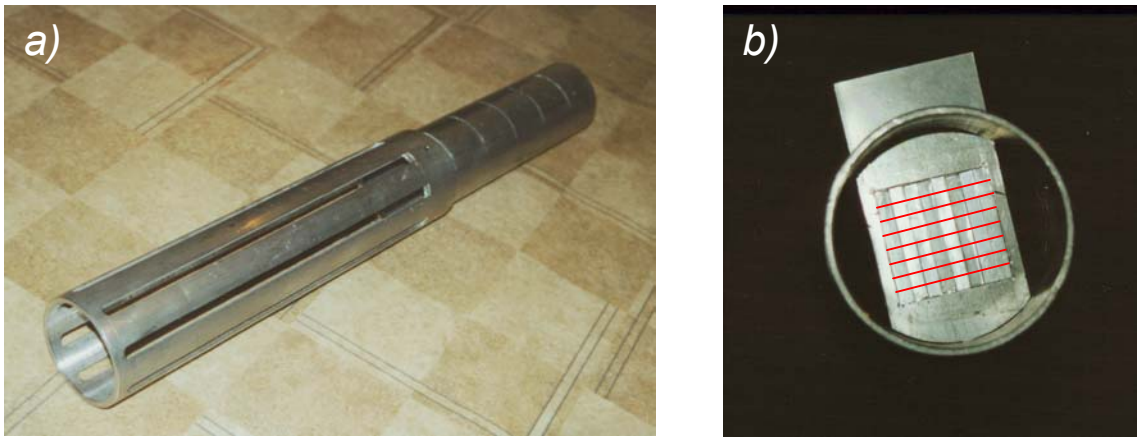

Photo 1. a) Pb target and sample holder, b) matrix of Al monitors for beam profile measurement in the position of irradiation. Black lines mark the cutting of aluminium strips after irradiation.

The irradiated samples and monitors were counted without background shielding in a typical vertical counting geometry with the use of HPGe coaxial detector ORTEC GEM-20180-p. They were placed 5 or 10 cm above the detector.

3. MONITORING OF THE PROTON BEAM

The results obtained in three irradiations are discussed here below. The characteristic of each of them is given in Table I. The total number of protons during irradiation was monitored with the use of ^{27}Al(p,x)^{22}Na reaction, while the activity from ^{27}Al(p,x)^{24}Na reaction was applied for the assessment of proton beam profile (Fig.3).

Table I. Irradiation conditions applied in the experiments.

Irradiation number	Target Length [cm]	Sample positions/ irradiation time	Irradiated samples	Number of protons [10^{13} p] calculated from the ^{22}Na activity of Al foil and reaction cross section [3]
1	50*	Front & back / 21 m	Al, Fe, Cu, Nb, Pb, Mg, Cr, Mn, Ta, W (front), Ni, Bi (back)	2.03 ± 0.12
2	31	In target / 10 h	Pb	2.14 ± 0.16
3	31	In target / 9 h	Pb	26.3 ± 1.9
3	31	Front & back / 9 h	Zr, Fe, Cu, Nb, Pb, Mg, Cr, Mn, Ta, W, Ni, Bi	26.3 ± 1.9

*/ earlier experiment described in [1]

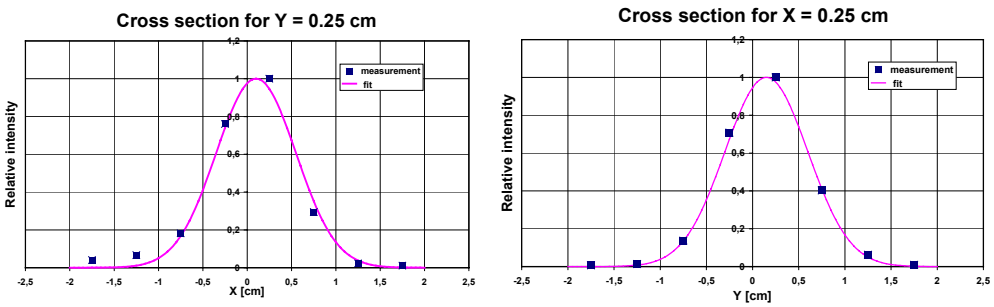

Fig. 3. Shape of the measured average proton beam profile and fitted two-dimensional Gauss distribution with standard deviation equal to 4.5 mm.

4. DETERMINATION OF ACTIVITY

To calculate the correct absolute activity of a given radionuclide from measured γ spectrum one should determine not only the intensity and profile of the proton beam but also the counting efficiency characteristic for the applied detection conditions. This was particularly important for the large Pb disc samples (Φ80×1 mm) irradiated in a mixed proton and neutron field inside the Pb target. In this case one should take into account such effects occurring during sample counting as: non point-source geometry, absorption of γ-rays in lead sample and non-uniform distribution of activity within sample different almost for each sample. The problem was solved by measurements of spectra of certified point sources and computations of: point source efficiency curve for the used detector (MCNP), activity distribution in samples (LAHET) and real measurement efficiency curves for various activity distributions (MCNP). The results are presented in Figures 4-6. In the Fig. 4 one can see the degree of accuracy of computer simulation of the point-source geometry efficiency. Considering this result satisfactory efficiencies for real counting conditions of large Pb samples were calculated (Fig.6) based on the calculated activity distribution in samples (Fig.5).

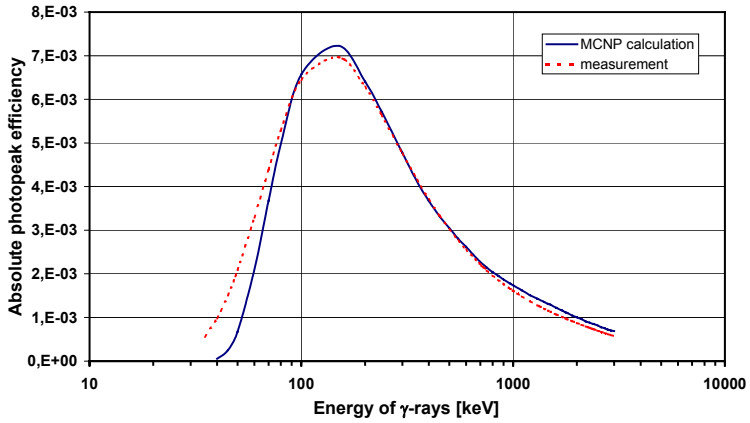

Fig. 4. Measured and computed (MCNP) absolute efficiency of HPGe coaxial detector for point source counting geometry.

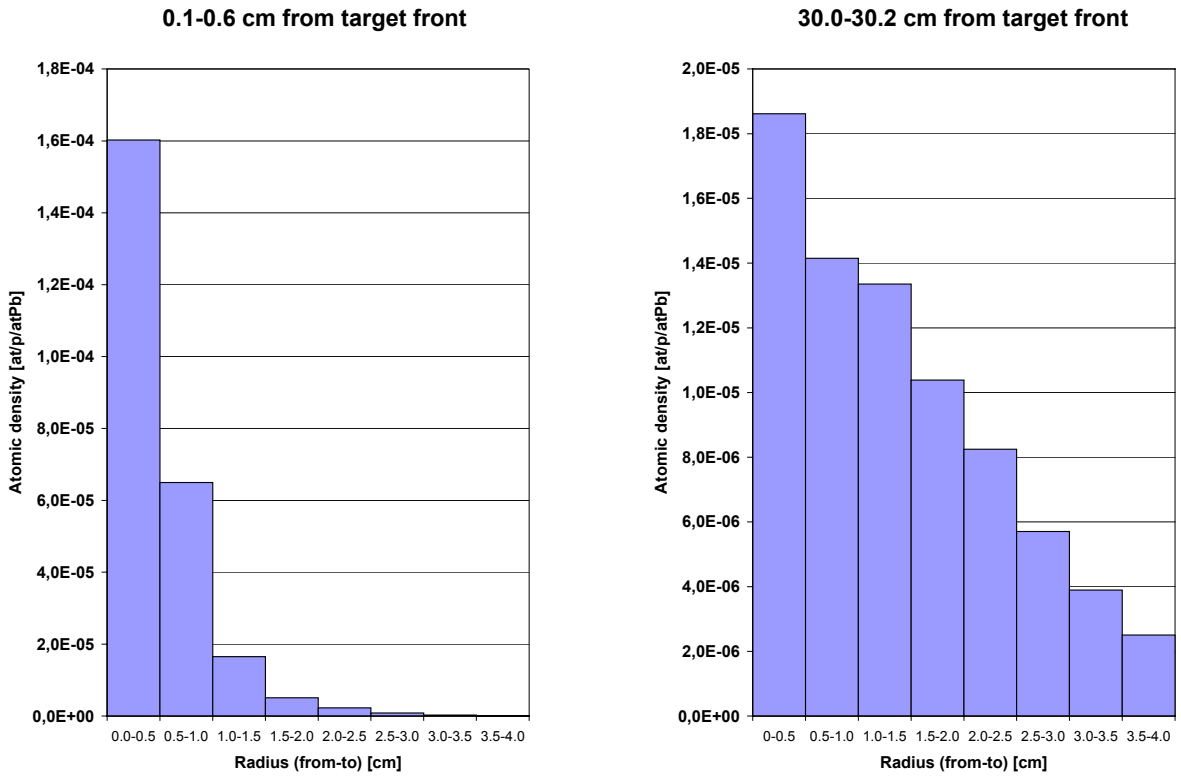

Fig. 5. Calculated (LAHET) radial distributions of ^{205}Bi concentration in Pb samples at the front and at the end of target.

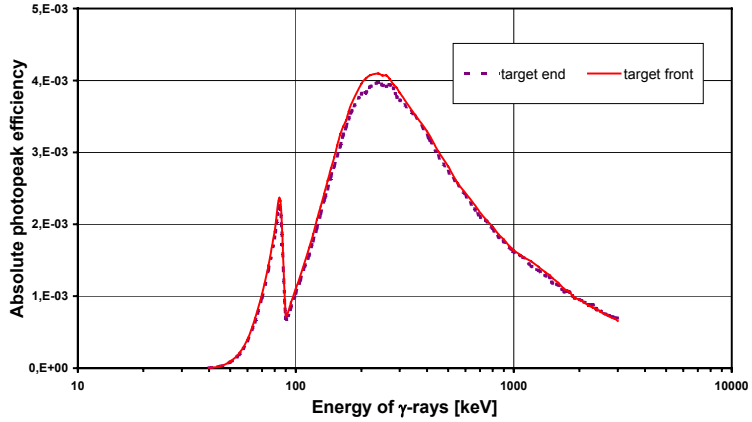

Fig. 6.

Calculated (MCNP) absolute photopeak detection efficiency for the real counting geometry of large Pb samples. Taken into account different distributions in front and at the end of target.

IV. RESULTS

The gamma spectra of irradiated samples were measured several times. For samples placed behind the Pb target the respective activities are rather low and difficult for a reliable measurement. Nevertheless several nuclides were identified in Bi samples after a long counting (5-9 h). They are presented in Table II. Measurements of long-lived nuclides are continued.

Table II. Activity generated in the Bi sample placed behind a lead target.

Target length [cm]	50	31	
No of protons[E13]	2.03 ± 0.12	26.3 ± 1.9	
Decay time [h] =	9,5	12,2	137
Nuclide /$T_{1/2}$	Activity [10^{-37}Bq/p/at Bi]		
^{207}Bi/31.55y			2,02 ± 0,15*
^{206}Bi/6.243d	175 ± 17	2420 ± 110	1360 ±110
^{205}Bi /15.31d		942 ± 80	745 ± 60
^{204}Bi /11.22h	621 ± 42	1730 ± 130	
^{203}Bi /11.76h	778 ± 72	1490 ± 210	
^{203}Pb /51.873h		1970 ± 190	
^{201}Pb /9.33h	710 ± 50	826 ± 110	
^{200}Pb /21.5h	145 ± 18	647 ± 210	
^{203}Hg /46.612d		464 ± 40	429 ± 40
^{202}Tl /12.23d			40 ± 9
^{201}Tl /72.912h			263 ± 70
^{200}Tl /26.1h	173 ± 20	1540 ± 150	150 ± 14
^{199}Tl /7.42h	430 ± 60		

* measured after a long decay (150 d) and recalculated to the end of irradiation

The other part of results regards the Pb samples irradiated inside the target. From the nuclides identified in γ-spectra measured for these samples some were selected for quantitative evaluation. Examples of the results are presented in Table III and on Figures 7-9.

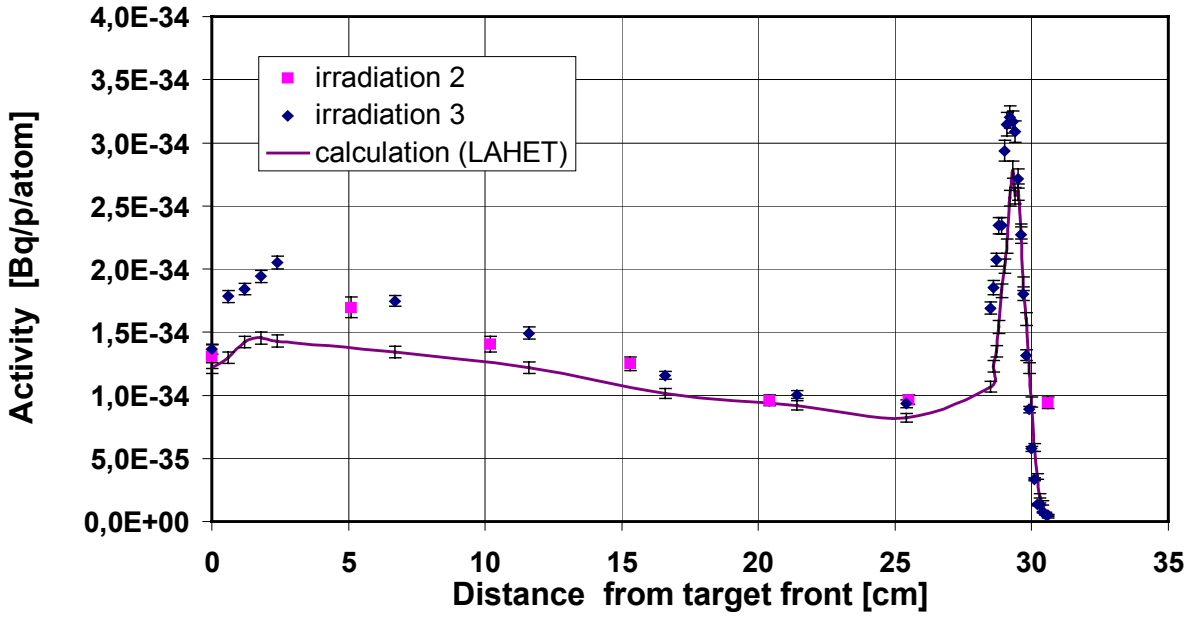

Fig. 7. Distribution of ^{205}Bi activity along the Pb target

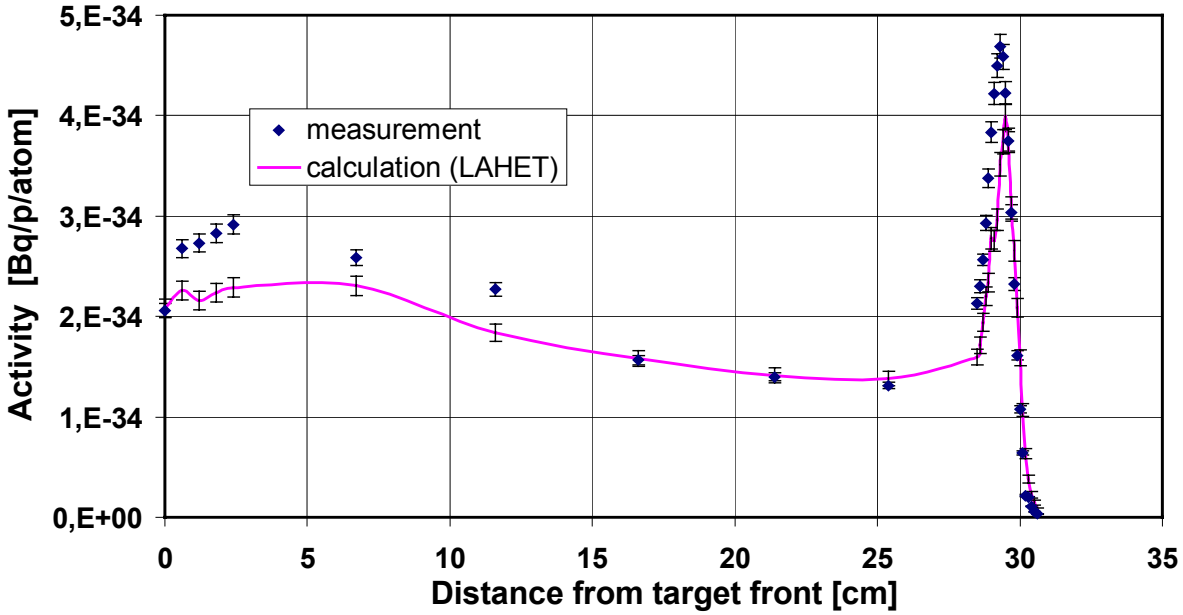

Fig. 8. Distribution of ^{206}Bi activity along the Pb target

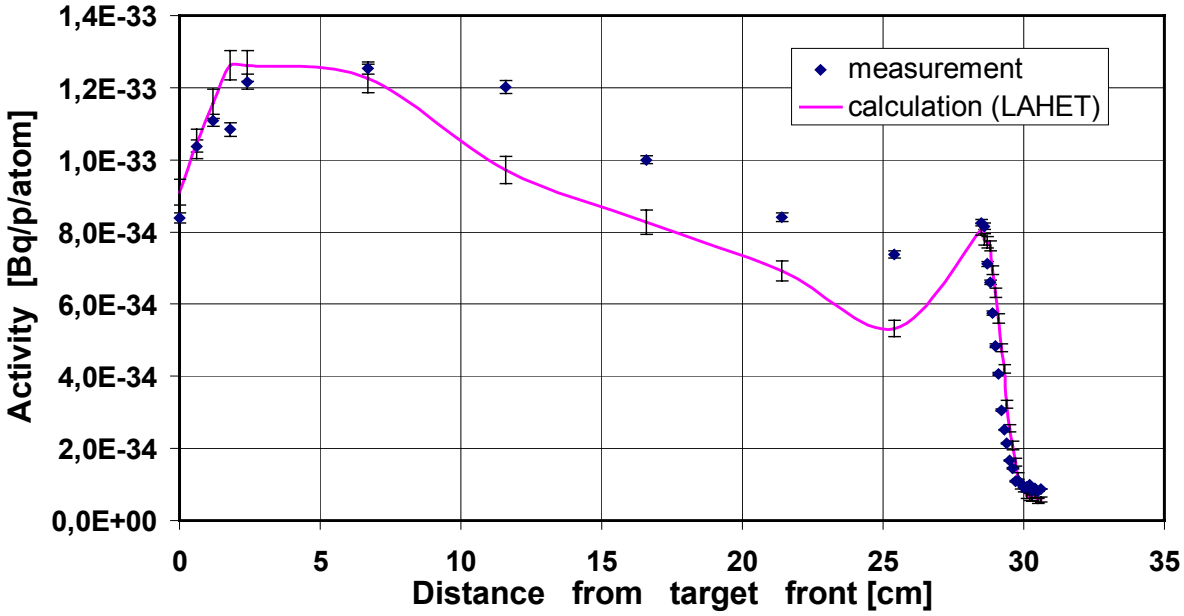

Fig. 9. Distribution of ^{201}Tl activity along the Pb target

Table IIIa. Activity determined in Pb samples
(at the end of 9h irradiation with proton fluence 2.6E14 ± 1.6E13 in samples of Φ80mm ×1 mm).

Sample depth in the target	^{206}Bi		^{205}Bi	
[cm]	Activity	Uncertainty*	Activity	Uncertainty*
	[Bq/proton/Pb atom]			
0.0	2.06E-34	6.80E-36	1.36E-34	3.52E-36
0.6	2.67E-34	9.00E-36	1.78E-34	4.84E-36
1.2	2.73E-34	9.04E-36	1.84E-34	4.54E-36
1.8	2.83E-34	9.33E-36	1.94E-34	4.81E-36
2.4	2.91E-34	9.61E-36	2.05E-34	5.12E-36
6.7	2.58E-34	8.00E-36	1.75E-34	4.15E-36
11.6	2.27E-34	6.81E-36	1.49E-34	4.71E-36
16.6	1.57E-34	4.54E-36	1.16E-34	3.04E-36
21.4	1.40E-34	4.16E-36	1.00E-34	3.10E-36
25.4	1.31E-34	3.42E-36	9.34E-35	3.11E-36
28.5	2.13E-34	5.57E-36	1.69E-34	4.78E-36
28.6	2.30E-34	6.36E-36	1.85E-34	5.73E-36
28.7	2.56E-34	5.83E-36	2.07E-34	5.14E-36
28.8	2.93E-34	7.53E-36	2.34E-34	6.40E-36
28.9	3.38E-34	9.17E-36	2.34E-34	6.40E-36
29.0	3.83E-34	1.05E-35	2.94E-34	7.98E-36
29.1	4.22E-34	1.11E-35	3.14E-34	9.27E-36
29.2	4.50E-34	1.17E-35	3.20E-34	8.92E-36
29.3	4.69E-34	1.18E-35	3.16E-34	8.80E-36
29.4	4.58E-34	1.23E-35	3.09E-34	8.61E-36
29.5	4.23E-34	1.11E-35	2.72E-34	7.56E-36
29.6	3.74E-34	9.67E-36	2.27E-34	6.34E-36
29.7	3.03E-34	8.06E-36	1.80E-34	5.37E-36
29.8	2.32E-34	6.21E-36	1.32E-34	4.15E-36
29.9	1.61E-34	4.60E-36	8.87E-35	2.76E-36
30.0	1.08E-34	3.37E-36	5.77E-35	2.01E-36
30.1	6.41E-35	1.98E-36	3.35E-35	1.28E-36
30.2	2.17E-35	8.71E-37	1.35E-35	8.12E-37
30.3	1.98E-35	6.99E-37	1.38E-35	6.78E-37
30.4	1.10E-35	4.98E-37	7.33E-36	5.65E-37
30.5	5.34E-36	3.37E-37	5.42E-36	4.31E-37
30.6	3.30E-36	2.36E-37	5.34E-36	4.53E-37

*/ one standard deviation of the number of counts

Table IIIb. Activity determined in Pb samples
(at the end of 9h irradiation with proton fluence 2.6E14 ± 1.6E13 in samples of Φ80mm ×1 mm).

Sample depth in the target	^{200}Tl		^{201}Tl	
[cm]	Activity	Uncertainty*	Activity	Uncertainty*
	[Bq/proton/Pb atom]			
0	5,86E-34	1,37E-35	8,38E-34	4,77E-35
0,6	7,19E-34	1,68E-35	1,04E-33	8,02E-35
1,2	7,68E-34	1,69E-35	1,11E-33	8,65E-35
1,8	6,54E-34	1,84E-35	1,08E-33	9,12E-35
2,4	7,02E-34	2,00E-35	1,22E-33	8,97E-35
6,7	8,55E-34	1,70E-35	1,25E-33	8,83E-35
11,6	8,14E-34	1,72E-35	1,20E-33	6,92E-35
16,6	5,36E-34	1,05E-35	1,00E-33	4,85E-35
21,4	5,73E-34	1,16E-35	8,41E-34	3,61E-35
25,4	5,34E-34	1,03E-35	7,37E-34	3,83E-35
28,5	4,89E-34	8,88E-36	8,26E-34	3,07E-35
28,6	4,41E-34	8,95E-36	8,15E-34	3,21E-35
28,7	3,65E-34	6,41E-36	7,11E-34	2,73E-35
28,8	3,20E-34	6,14E-36	6,61E-34	2,64E-35
28,9	2,56E-34	5,68E-36	5,75E-34	2,60E-35
29	2,03E-34	4,81E-36	4,84E-34	1,91E-35
29,1	1,60E-34	3,58E-36	4,06E-34	1,67E-35
29,2	1,17E-34	2,79E-36	3,06E-34	1,55E-35
29,3	1,24E-36	3,28E-37	2,51E-34	1,24E-35
29,4	7,39E-35	2,06E-36	2,15E-34	9,39E-36
29,5	6,23E-35	1,64E-36	1,66E-34	5,87E-36
29,6	5,61E-35	1,46E-36	1,45E-34	5,65E-36
29,7	4,85E-35	1,28E-36	1,09E-34	4,56E-36
29,8	4,59E-35	1,19E-36	1,11E-34	4,60E-36
29,9	4,53E-36	7,82E-37	1,03E-34	5,57E-36
30	4,22E-35	1,29E-36	9,18E-35	3,12E-36
30,1	3,21E-36	5,73E-37	9,36E-35	4,84E-36
30,2	3,17E-36	5,29E-37	9,85E-35	4,69E-36
30,3	3,53E-36	5,30E-37	8,28E-35	5,02E-36
30,4	3,55E-36	4,44E-37	8,89E-35	3,28E-36
30,5	3,59E-37	1,28E-37	8,16E-35	4,05E-36
30,6	6,81E-36	7,30E-37	8,73E-35	3,92E-36

*/ one standard deviation of the number of counts

4. DISCUSSION OF RESULTS AND CONCLUSIONS

1. The distributions of isotope activity along the lead target, both the experimentally determined and the ones computed in LAHET simulations, show a peak near the end of the beam proton range. The maximum results both from the energy spectrum of protons, changing with distance passed in lead

(Fig.10), and from the shape of the excitation function of respective reactions (Fig.11). These distributions for ^{205}Bi and ^{206}Bi are reproduced in LAHET calculations.

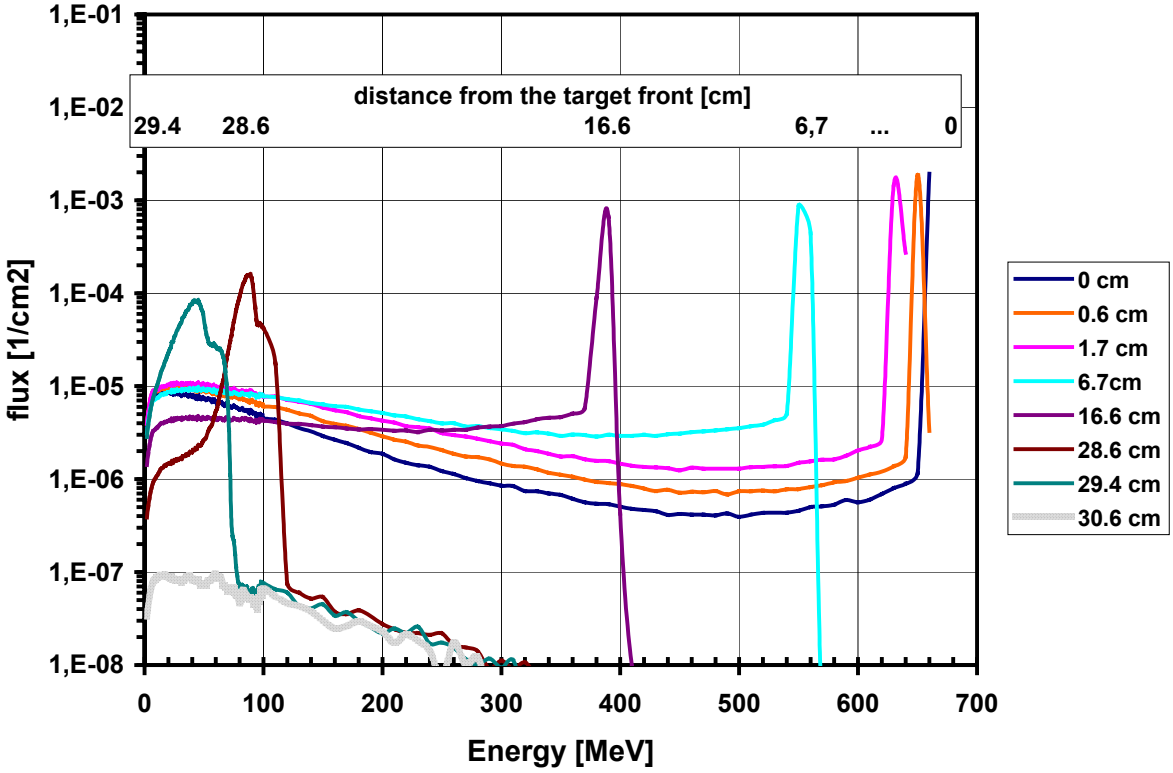

Fig. 10. Proton spectra in Pb samples (MCNPX)

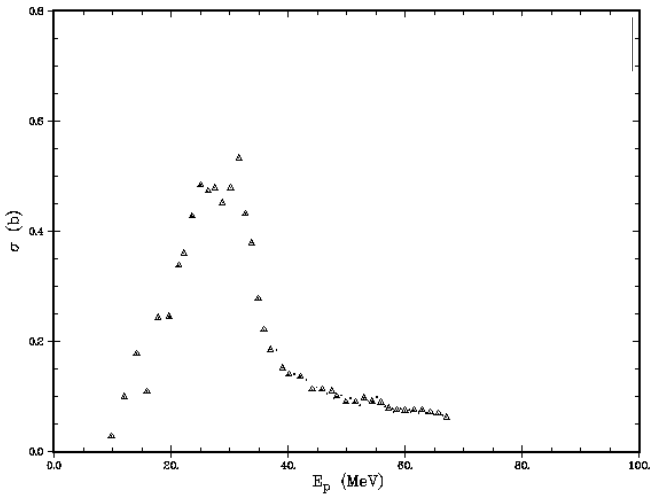

Fig. 11. Cross section for reaction Pb(p,xn)^{206}Bi [4].

The calculated activities agree with the measured ones at the target front and near the distribution peak while the intermediate results slightly differ. For reactions leading to ^{201}Tl and ^{200}Tl, which have higher threshold energy, position of the maximum is shifted back (towards the target front). It could not be well determined in our measurement (which was designed for assessment of ^{206}Bi

and ^{205}Bi distributions). Nevertheless, the right side of the peak and the rest of distribution were measured sufficiently well. Again, the calculated and measured activities agree at the target front and on the right side of peak while the intermediate results differ considerably. It is planned to continue experiments for these nuclides.

2. A good agreement of calculation and measurement at the target front and near the end of primary proton range is observed. It results most probably from the fact that in both cases the activation comes mainly from reactions induced by the primary protons and for their energy ranges where the applied reaction models work properly. On the other hand in between increases the role of secondary protons and neutrons and their transport in lead. Thus, one can suppose that in this case low energy neutron (< 20 MeV) induced production, not taken into account in calculations, and worse performance of respective models is the reason of the discrepancy.
3. In the samples of Bi placed behind the primary proton range several neutron induced reaction products were observed. The results obtained for two Pb targets of 50 cm and 31cm length are compared. Production yields of identified isotopes are up to 14 times higher for the shorter target. Respective computer calculations are under way. The measured activity of ^{207}Bi ($T_{1/2}$=31.55y), however low here, may reach high values in full scale installations.

ACKNOWLEDGEMENTS

The Polish State Committee for Scientific Research supported the present work under the project SPUB-M/5 PR UE/DZ 19/2001-2003.
Thanks are due to Prof. V.S. Buttsev for supplying parts of the applied lead target, to Drs. A.G. Molokanov and I.V. Mirokhin for operation of the Phasotron and all the help given during the experiment and to Dr V.G. Sandukovski for landing the equipment applied for gamma spectrometry.

REFERENCES

1. J. Janczyszyn et al., "Experimental Assessment of Radionuclide Production in Materials Near to the Spallation Target", *Proc. of the Conf. "Accelerator Applications/Accelerator Driven Transmutation Technology and Applications" (AccApp/ADTTA'01)*, Reno, Nevada, November 12-15, 2001 (in press).
2. V. P. Bamblevski et al., "The Investigation of the Radiation Field Around the Thick Lead Target Irradiated by the 650 MeV Protons. Part 1" *JINR Report* **E1- 2000 - 307**, Dubna (2000).
3. T. N. Tadeucci, et al., "Total cross sections for production of ^{7}Be, ^{22}Na, and ^{24}Na in p+^{7}Li and p+^{27}Al reactions at 495 and 795 MeV", *Phys.Rev.* **C 55**, 1551 (1997).
4. M. C. Lagunas-Solar et al., "Cyclotron Production of No-Carrier-Added ^{206}Bi (6.24 d) and ^{205}Bi (15.31 d) as Tracers for Biological Studies and for the Development of Alpha-Emitting Radiotherapeutic Agents", *J. App. Rad. Isot*. **38**, 129 (1987).